15. D. N. Lee, L. Phung, J. Stewart, R. Landick, *J. Biol. Chem.* **265**, 15145–15153 (1990).
16. M. Dangkulwanich *et al.*, *eLife* **2**, e00971 (2013).
17. L. Bai, A. Shundrovsky, M. D. Wang, *J. Mol. Biol.* **344**, 335–349 (2004).
18. V. R. Tadigotla *et al.*, *Proc. Natl. Acad. Sci. U.S.A.* **103**, 4439–4444 (2006).
19. N. Sugimoto *et al.*, *Biochemistry* **34**, 11211–11216 (1995).
20. J. Zhou, K. S. Ha, A. La Porta, R. Landick, S. M. Block, *Mol. Cell* **44**, 635–646 (2011).
21. Y. Zhang *et al.*, *Science* **338**, 1076–1080 (2012).

ACKNOWLEDGMENTS

This work was supported by NIH grants GM041376 (R.H.E.), GM088343 (B.E.N.), and GM096454 (B.E.N.). Reads are deposited in the Sequence Read Archive (accession SRP039384).

SUPPLEMENTARY MATERIALS

www.sciencemag.org/content/344/6189/1285/suppl/DC1
Materials and Methods
Figs. S1 to S9
Tables S1 to S12
References (*22*–*32*)

17 March 2014; accepted 2 May 2014
10.1126/science.1253458

DISEASE ECOLOGY

Ecological and evolutionary effects of fragmentation on infectious disease dynamics

Jussi Jousimo,[1]* Ayco J. M. Tack,[1]* Otso Ovaskainen,[1] Tommi Mononen,[1,2] Hanna Susi,[1] Charlotte Tollenaere,[1] Anna-Liisa Laine[1]†

Ecological theory predicts that disease incidence increases with increasing density of host networks, yet evolutionary theory suggests that host resistance increases accordingly. To test the combined effects of ecological and evolutionary forces on host-pathogen systems, we analyzed the spatiotemporal dynamics of a plant (*Plantago lanceolata*)–fungal pathogen (*Podosphaera plantaginis*) relationship for 12 years in over 4000 host populations. Disease prevalence at the metapopulation level was low, with high annual pathogen extinction rates balanced by frequent (re-)colonizations. Highly connected host populations experienced less pathogen colonization and higher pathogen extinction rates than expected; a laboratory assay confirmed that this phenomenon was caused by higher levels of disease resistance in highly connected host populations.

Although infectious diseases pose serious threats to human health and food security, pathogens are also a fundamental component of natural biodiversity (*1*, *2*). Infection prevalence fluctuates through space and time in natural plant-pathogen associations (*3*–*5*), but there is little evidence of devastating epidemics in native interactions. This is in stark contrast to the boom-and-bust dynamics of many fungal pathogens attacking commercially important crops under agricultural settings (*6*, *7*) and epidemics caused by introduced species (*8*). With most of the focus in epidemiology targeted toward understanding conditions generating infectious disease outbreaks (*9*–*11*), the mechanisms that enable long-term disease persistence in wild communities remain elusive.

Spatially explicit metapopulation theory has identified habitat size and connectivity to other habitat patches as the key parameters affecting species distributions (*12*). The limited data available have confirmed metapopulation theory to be relevant also for disease dynamics, with colonizations and extinctions of local host populations generating the observed patterns of infection (*13*). Far less is known about how evolutionary dynamics vary through space and what the resulting effects on disease dynamics are (*14*). There is substantial theory demonstrating that the spatial scale of host-pathogen interactions and resulting rates of gene flow are critical for how coevolutionary dynamics play out between hosts and their pathogens (*15*, *16*). Hence, although host availability for pathogens increases with increasing density of host networks, the evolutionary potential of host populations may also change as a function of connectivity. Increased host gene flow into the local populations generates higher variation in resistance, allowing resistance to be selected for (*17*, *18*). A comparison across species found the relative rate of gene flow in hosts versus parasites to be the strongest predictor of pathogen local adaptation to host resistance. When host dispersal rates exceeded those of their parasites, the potential for parasite maladaptation emerged (*19*). However, such species-level approaches provide little insight into how coevolutionary dynamics and resulting infectious disease dynamics are played out across the spatially heterogeneous landscapes that most species inhabit. Indeed, the spatial and the genetic complexities that natural host-pathogen interactions support have rendered epidemiological predictions challenging in wild communities, yet identifying the effect of such complexity on epidemiological dynamics may provide key insights into the battle against diseases.

To understand how spatial and evolutionary processes interact to shape disease dynamics, we analyzed the spatial and environmental factors that drive metapopulation dynamics of an obligate fungal pathogen occupying a highly fragmented host population network. In our analyses, we targeted the three key steps of metapopulation dynamics: presence-absence of disease within local host populations (i.e., occupancy); colonization by the pathogen of previously unoccupied host populations; and extinction, whereby a pathogen population previously found infecting a local host population is deemed lost. We also analyzed factors affecting within-population abundance of disease. Our spatial variables included host population size, presence of road, host population connectivity (S^H), and pathogen population connectivity at the beginning (S^P) and the end (S^M) of epidemics. The environmental variables were percentage of dry host plants within populations, habitat boundary type, light availability, and precipitation in July and August. We used a hierarchical spatiotemporal Bayesian logistic regression model that allows estimation of the residual spatial and temporal autocorrelation.

Our data were collected from *Podosphaera plantaginis*, a specialist powdery mildew naturally infecting *Plantago lanceolata* in the Åland archipelago, southwestern Finland. *P. lanceolata* is an obligate outcrossing perennial herb that reproduces both sexually and clonally via side rosettes. The pollen of *P. lanceolata* is wind-dispersed, and seeds typically drop close to the mother plant. In Åland, the host populations are highly fragmented, forming a network of several thousand populations spanning an area of about 50 km by 70 km. Locations of the local *P. lanceolata* populations in the Åland Islands have been annually mapped since the 1990s. Because of clonal reproduction and a seed bank, host populations rarely go extinct, and hence the spatial configuration of the host populations remains relatively constant (*12*). Visible signs of infection by *P. plantaginis* begin to appear in late June in those host populations where the pathogen has successfully survived the winter as resting spores. The resting spores remain attached to the senescent host leaves throughout the winter, and in the spring the spores may reinfect the same host plant or new host plants in close vicinity (*20*, *21*). The epidemic starts from these initial disease foci when the pathogen is transmitted among hosts by clonally produced dispersal spores that are passively carried by wind (*5*, *22*). Some six to eight clonally produced generations follow one another in quick

[1]Metapopulation Research Group, Department of Biosciences, University of Helsinki, Post Office Box 65 (Viikinkaari 1), FI-00014 University of Helsinki, Helsinki, Finland. [2]Department of Biomedical Engineering and Computational Science, Aalto University School of Science, FI-00076 Aalto, Finland. *These authors contributed equally to this work. **†Corresponding author. E-mail: anna-liisa.laine@helsinki.fi**

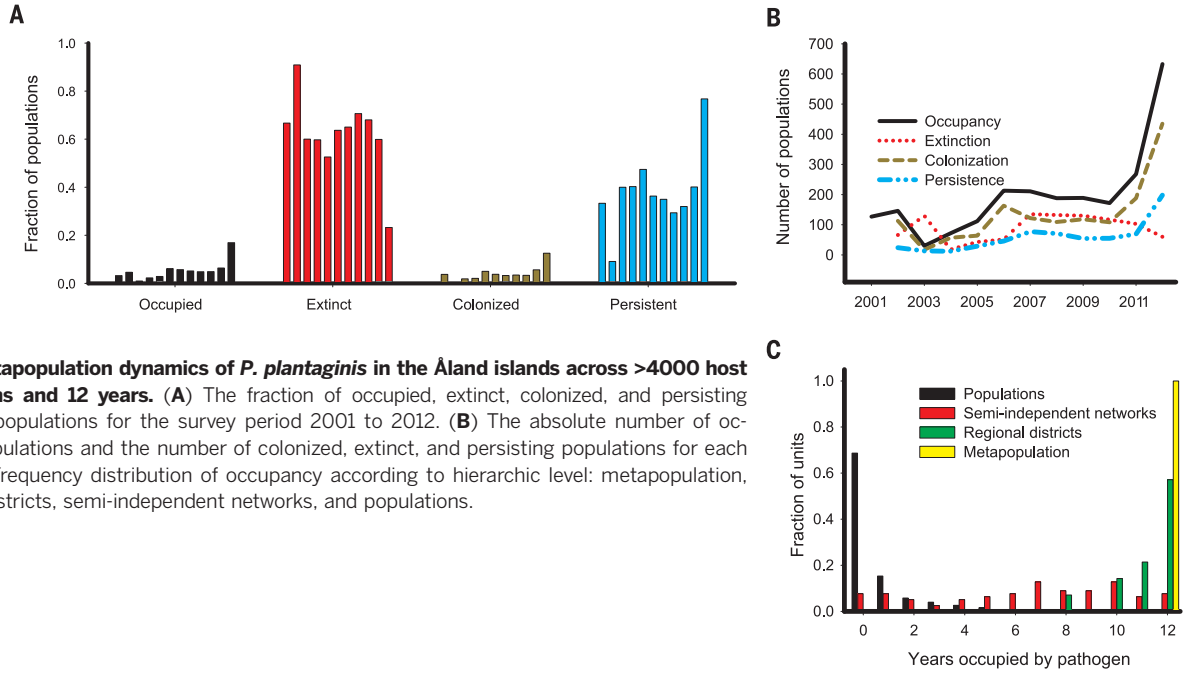

Fig. 1. Metapopulation dynamics of *P. plantaginis* in the Åland islands across >4000 host populations and 12 years. (**A**) The fraction of occupied, extinct, colonized, and persisting pathogen populations for the survey period 2001 to 2012. (**B**) The absolute number of occupied populations and the number of colonized, extinct, and persisting populations for each year. (**C**) Frequency distribution of occupancy according to hierarchic level: metapopulation, regional districts, semi-independent networks, and populations.

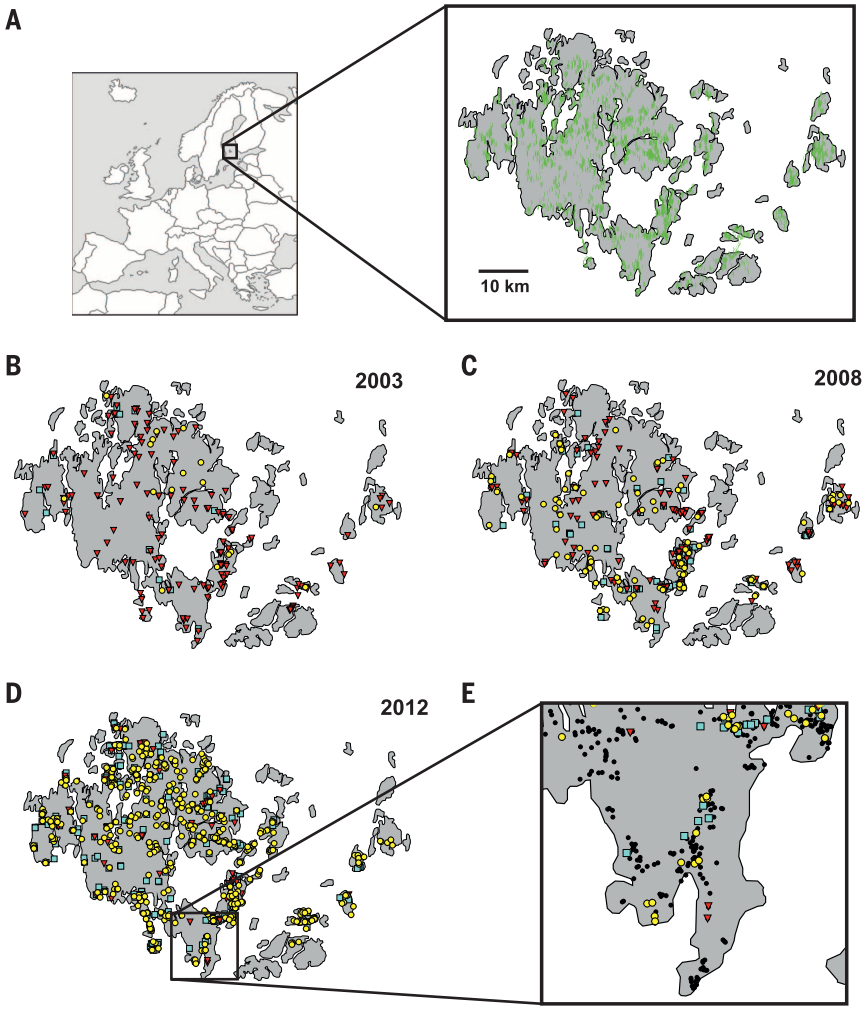

Fig. 2. Spatial distribution of host and pathogen populations. (**A**) Distribution of the host populations. (**B** to **D**) Colonized (yellow circles), extinct (red triangles), and persistent (blue squares) pathogen populations for a year with low, average, and high occupancy, respectively. (**E**) Fine-scale extinction-colonization dynamics in the regional district of Lemland in 2012, where black dots represent uncolonized host populations.

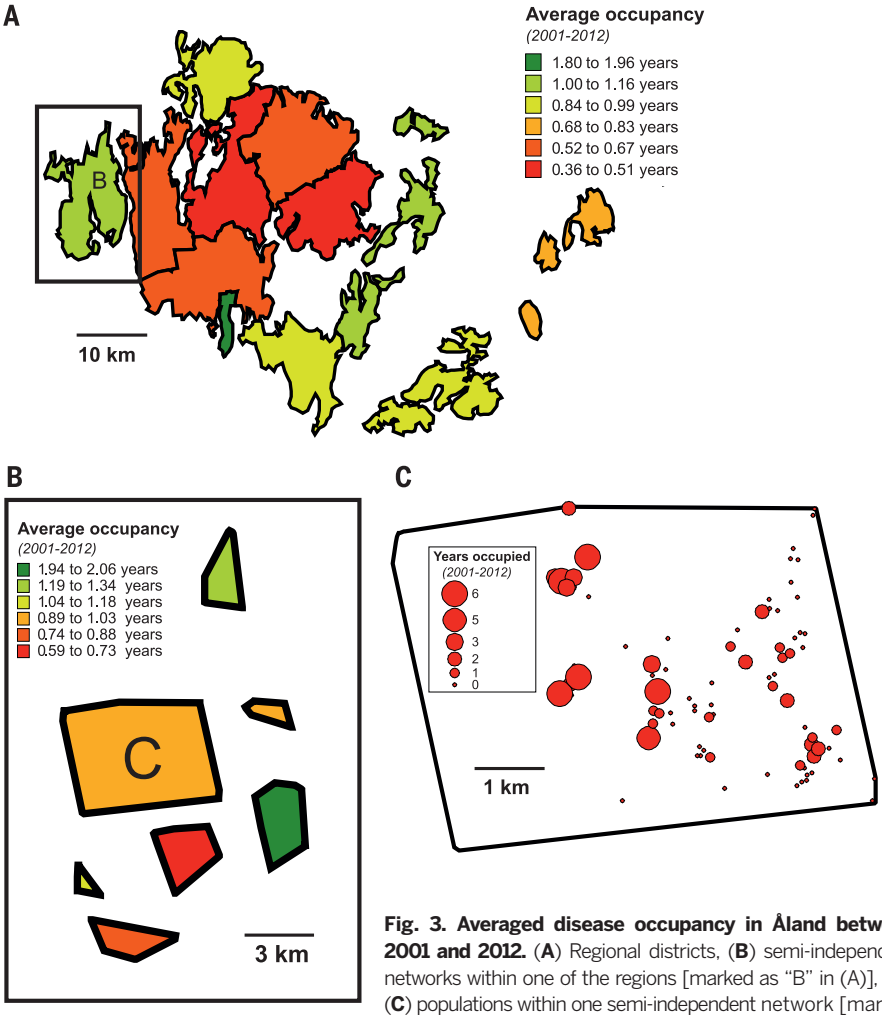

Fig. 3. Averaged disease occupancy in Åland between 2001 and 2012. (**A**) Regional districts, (**B**) semi-independent networks within one of the regions [marked as "B" in (A)], and (**C**) populations within one semi-independent network [marked as "C" in (B)].

succession, and, as a consequence, infection spreads within (*22*) and between host populations (*5*). By September, weather conditions turn unfavorable to pathogen transmission, and the epidemic spread ceases. At this time, since 2001, the entire host population network is surveyed for the presence-absence of the pathogen. This host-pathogen interaction is highly amenable to large-scale ecological studies, because infection is visually conspicuous (fig. S1) and the disease cycle lacks extended latency periods. Hence, field surveys at the end of epidemics yield a direct measure of host population size and disease prevalence within host populations, and the extinction-colonization dynamics of the pathogen can be inferred from these snapshot data by comparing the infection status of a given host population to its infection status in the previous year.

We complemented our analysis of spatial disease dynamics by assessing pathogen resistance through inoculation trials where host plants are challenged with fungal strains. The experiment consisted of 22 host populations representing different degrees of S^H. In the interaction between *P. lanceolata* and *P. plantaginis*, disease resistance is strain-specific, with the same host genotype blocking infection by some strains of the pathogen while being susceptible to others (*23*), and there is considerable variation among host individuals and populations in their degree of resistance (*24*). The obligate pathogen can only establish on susceptible hosts, and hence variation in resistance is expected to play a fundamental role in determining disease dynamics (*24*). Resistance should be favored because infected hosts suffer increased mortality in wild populations (*24*, *25*). Ongoing studies suggest that resistance is costly for *P. lanceolata*, potentially explaining why this trait is so variable in Åland.

Our results show that in any one year the pathogen occupies only a small fraction of the available plant populations, generally ranging from 1.1 to 6.7%, with an exceptionally high occupancy in 2012 (16.9%; Fig. 1, A and B). The turnover of the pathogen populations is extremely high, because a large fraction of the pathogen populations (23.3 to 90.9%) go extinct every year (Figs. 1 and 2, B to E), predominantly during the critical overwintering stage (*21*). As a consequence, there is a major role for colonizations in maintaining the pathogen population regionally by counterbalancing the high extinction rates (Fig. 1, A and B). How these rates vary determines the annual disease occupancy levels (Figs. 1, A and B, and 2, B to E). Overall, our data show strong variation in the prevalence of the pathogen across several spatial scales (Figs. 1C and 3). Notably few host populations have been occupied for multiple years, and only a single host population has been occupied during the entire 12-year survey period (Fig. 1C). Instead, pathogen persistence takes place at regional district (Figs. 1C and 3A) and network levels (Figs. 1C and 3B).

The spatiotemporal Bayesian logistic regression model revealed the importance of spatial factors on disease dynamics at the metapopulation level as well as on local abundance (Table 1;

Table 1. Environmental and spatial drivers of pathogen metapopulation dynamics and within population abundance analyzed with a Bayesian spatiotemporal logistic regression model. Mean parameter posterior estimate and its posterior standard error are shown for each factor for models analyzing the presence-absence of the pathogen (PA), the colonization of unoccupied (COL), and the extinction of occupied (EXT) plant populations. Population abundance (ABUND) was modeled by using categorical abundance data collected in autumn 2012. Nonsignificant (NS) parameters were removed from the models based on deviance information criterion. Patch shadow has three ordered levels, ranging from full exposure to sunlight (1) to shadow during most of the day (3).

Parameter	PA	COL	EXT	ABUND
Intercept	−4.2 ± 0.9	−3.9 ± 0.9	0.48 ± 0.36	2.02 ± 0.09
Metapopulation configuration				
Spatial factors				
Host population area (*A*)	0.30 ± 0.05	0.26 ± 0.06	−0.27 ± 0.19	NS
S^H	−1.2 ± 0.4	−0.82 ± 0.29	0.38 ± 0.16	−0.16 ± 0.13
Road presence	1.2 ± 0.1	1.2 ± 0.1	−0.43 ± 0.11	0.13 ± 0.07
S^M	not fitted	NS	−1.0 ± 0.2	not fitted
S^P	not fitted	0.08 ± 0.10	NS	not fitted
Environmental factors				
Plant dryness	NS	NS	NS	0.18 ± 0.07
Habitat boundary type	NS	NS	NS	0.47 ± 0.31
Patch shadow, linear	−0.77 ± 0.14	−0.89 ± 0.19	NS	NS
Patch shadow, quadratic	−0.05 ± 0.09	−0.14 ± 0.11	NS	NS
July rainfall	NS	NS	NS	0.11 ± 0.10
August rainfall	−0.25 ± 0.09	−0.13 ± 0.11	NS	NS

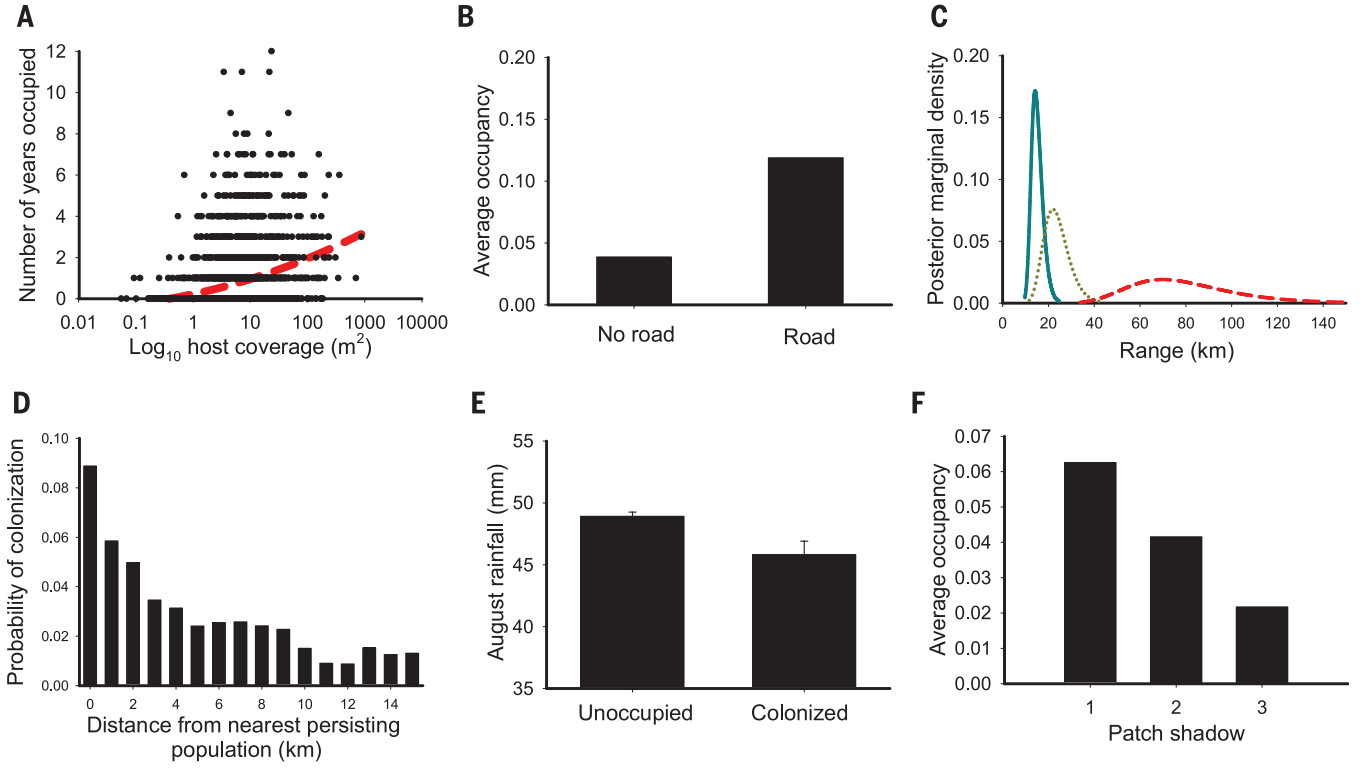

Fig. 4. The impact of environmental and spatial variables on disease dynamics. (**A**) Plant population area (correlates with number of individuals) and (**B**) the presence of a road had a positive effect on population occupancy by the pathogen. In (A), a dashed red trend line is shown. (**C**) Posterior Bayesian estimates for the range parameter for occupancy (solid blue line), colonizations (yellow dotted line), and extinctions (dashed red line). (**D**) Probability of colonization of an unoccupied host population as a function of the distance to the nearest persisting pathogen population (up to 15 km) for all years. (**E**) Average August rainfall was higher in populations that remained unoccupied (uncolonized) than in populations that became colonized by the pathogen during 2011. Error bars indicate SEM. (**F**) Increasing patch shadow reduces the pathogen average occupancy.

Fig. 5. The impact of host network configuration on metapopulation dynamics and disease resistance. (**A**) Extinction probability of the pathogen populations in year 2012 from plant populations that were colonized in the previous year increased as a function of host population connectivity (generalized linear model: S^H; $F_{1,183}$ = 7.17, P = 0.008). (**B**) Host resistance was higher in well-connected than in isolated populations (linear model: $F_{1,21}$ = 4.63, P = 0.0437).

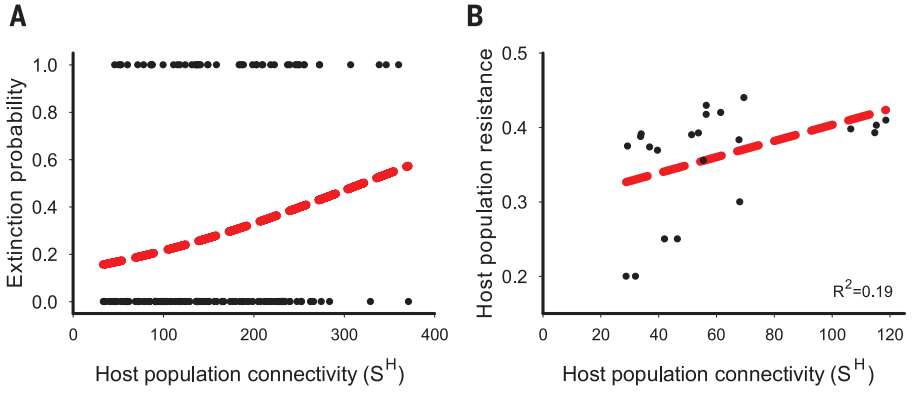

Fig. 4, A and B; tables S1 to S4; and figs. S2 to S5). As predicted by metapopulation theory (*12*), large host populations sustained higher colonization rates and lower extinction rates by the pathogen than did small host populations (Table 1 and Fig. 4A). Limited availability of large host populations is likely to be a key restricting factor of infection in this system. The colonization rate of the pathogen in any particular host population was affected by its spatial connectivity to other pathogen populations that had survived the winter that same year (S^P, Table 1), providing strong evidence for dispersal limitation with the majority of colonizations occurring within a radius of several kilometers from an occupied population (Fig. 4, C and D). Colonization happens predominantly over short distances, but there are infrequent longer-distance dispersal events that enable colonization of unoccupied areas (Fig. 4D) and are recognized to be important for large-scale dynamics of aerially transmitted fungi (*26*). Host populations that occurred along roadsides had significantly higher occupancy, abundance, and colonization probabilities and lower extinction probabilities of the pathogen (Table 1 and Fig. 4B). These results suggest that host plants growing in low densities along roadsides increase pathogen dispersal into the host populations (*5*), thus enhancing colonization and preventing extinction (Table 1).

The drivers of extinction and colonization dynamics appear to be distinct because none of the measured environmental factors explained extinction dynamics, whereas the transmission and establishment phase of infection were sensitive to abiotic variation (Table 1 and table S4). Rainfall in August, a critical transmission period for the pathogen, may have impeded transmission by removing spores from the air and from host leaves (Table 1 and Fig. 4E) (*27*). How large a proportion of the host population is shaded by surrounding forest had a negative effect on

occupancy and colonization rates, which may be explained by light, humidity, and temperature conditions (Table 1 and Fig. 4F). In contrast to colonizations, extinctions were characterized by a much higher range of spatial autocorrelation (Fig. 4C), suggesting the importance of large-scale (unmeasured) environmental variation in weather, such as snow cover, for this phase.

Last, our study confirms that host resistance increases as host population density increases, with direct effects on epidemiological dynamics. In contrast to predictions from metapopulation theory (*12*), isolated host populations were more frequently infected by the pathogen than host populations in dense networks (S^H, Table 1). Moreover, pathogen colonization rate decreased and extinction rate increased as a function of host population connectivity (Table 1). This trend was particularly pronounced for the extinction probability of the pathogen in recently colonized host populations (Fig. 5A). Our experimental challenge of 22 *P. lanceolata* populations with the pathogen confirmed that resistance was significantly higher in the highly connected than in the isolated host populations (Fig. 5B). *Plantago* populations rapidly evolve resistance against the powdery mildew (*25*), and potentially higher gene flow into well-connected host populations may result in increased evolutionary potential and hence may reduce the probability of pathogen establishment and persistence. In addition to putatively higher rates of gene flow between *P. lanceolata* populations in high-density networks, an alternative, although not mutually exclusive, hypothesis is that areas supporting high-density host networks may also represent high-productivity environments for the host. In high-quality environments, hosts may be able to invest more toward disease resistance than hosts growing in areas that are nutritionally limited (*28*), resulting in resistance aggregating in high-connectivity areas of the landscape. The study of how spatial connectivity affects host-pathogen coevolution has been predominantly theoretical (*16*, *17*), but, as shown in our work, variation in disease resistance among host populations may act as a powerful barrier against disease establishment in natural systems (*24*, *29*) and may stabilize coevolutionary dynamics (*30*).

Our study provides direct evidence of spatial structure having a profound effect on the ecology and evolution of disease dynamics in natural populations. Although comparable long-term and spatially explicit ecological and evolutionary data are lacking, we suggest that metapopulation structure and spatial heterogeneity at larger geographic scales may similarly drive antagonistic and mutualistic species interactions and their coevolutionary trajectories in a range of species interactions (*31*). Many factors explaining spatiotemporal variation in disease incidence across the metapopulation also explained within host population variation in disease abundance (Table 1), suggesting that incidence data at the metapopulation scale may be sufficient for understanding disease dynamics at finer spatial scales. With the majority of epidemiological studies targeted toward understanding the growth phase of epidemics, we argue that more research should be directed toward understanding the drivers behind disease persistence at low endemic levels and the between-epidemic phase. Spatial and environmental heterogeneity, combined with the evolution of increased host resistance in high density host networks, are likely to be important components that prevent runaway dynamics of infection in nature. These insights may provide a natural blueprint for managing emerging diseases, as well as managing outbreaks that threaten sustainable agriculture and human health.

REFERENCES AND NOTES

1. D. J. Bradley, G. S. Gilbert, J. B. H. Martiny, *Ecol. Lett.* **11**, 461–469 (2008).
2. E. T. Borer, E. W. Seabloom, C. E. Mitchell, A. G. Power, *Ecol. Lett.* **13**, 810–818 (2010).
3. D. L. Smith, L. Ericson, J. J. Burdon, *J. Ecol.* **99**, 634 (2011).
4. J. Antonovics, in *Ecology, Genetics, and Evolution of Metapopulations*, I. Hanski, O. Gaggiotti, Eds. (Academic Press, San Diego, CA, 2004), pp. 471–488.
5. A.-L. Laine, I. Hanski, *J. Ecol.* **94**, 217–226 (2006).
6. D. Cressey, *Nature* **493**, 587 (2013).
7. B. A. McDonald, C. Linde, *Annu. Rev. Phytopathol.* **40**, 349–379 (2002).
8. P. K. Anderson *et al.*, *Trends Ecol. Evol.* **19**, 535–544 (2004).
9. C. Viboud *et al.*, *Science* **312**, 447–451 (2006).
10. J. O. Lloyd-Smith, S. J. Schreiber, P. E. Kopp, W. M. Getz, *Nature* **438**, 355–359 (2005).
11. A. S. Siraj *et al.*, *Science* **343**, 1154–1158 (2014).
12. I. Hanski, *Metapopulation Ecology* (Oxford Univ. Press, Oxford, 1999).
13. B. Grenfell, J. Harwood, *Trends Ecol. Evol.* **12**, 395–399 (1997).
14. P. H. Thrall *et al.*, *Ecol. Lett.* **15**, 425–435 (2012).
15. S. Gandon, Y. Michalakis, *J. Evol. Biol.* **15**, 451–462 (2002).
16. S. Gandon, S. L. Nuismer, *Am. Nat.* **173**, 212–224 (2009).
17. U. Carlsson-Granér, P. H. Thrall, *Oikos* **97**, 97–110 (2002).
18. P. H. Thrall, J. J. Burdon, *Plant Pathol.* **51**, 169–184 (2002).
19. J. D. Hoeksema, S. E. Forde, *Am. Nat.* **171**, 275–290 (2008).
20. C. Tollenaere, A.-L. Laine, *J. Evol. Biol.* **26**, 1716–1726 (2013).
21. A. J. M. Tack, A.-L. Laine, *New Phytol.* **202**, 297–308 (2014).
22. O. Ovaskainen, A.-L. Laine, *Ecology* **87**, 880–891 (2006).
23. A.-L. Laine, *J. Evol. Biol.* **20**, 1665–1673 (2007).
24. A.-L. Laine, *J. Ecol.* **92**, 990–1000 (2004).
25. A.-L. Laine, *Proc. Biol. Sci.* **273**, 267–273 (2006).
26. J. K. M. Brown, M. S. Hovmøller, *Science* **297**, 537–541 (2002).
27. D. E. Aylor, *Annu. Rev. Phytopathol.* **28**, 73–92 (1990).
28. M. A. Duffy *et al.*, *Science* **335**, 1636–1638 (2012).
29. P. H. Thrall, J. Antonovics, *Can. J. Bot.* **73**, S1249 (1995).
30. E. Decaestecker, H. De Gersem, Y. Michalakis, J. A. M. Raeymaekers, *Ecol. Lett.* **16**, 1455–1462 (2013).
31. J. N. Thompson, *The Geographic Mosaic of Coevolution* (Univ. of Chicago Press, Chicago, 2005).

ACKNOWLEDGMENTS

We acknowledge I. Hanski, S. Ojanen, and M. Nieminen for organizing the large-scale field surveys in Åland and E. Meyke for managing the database. The numerous biology students who have participated in years 2001 and 2012 are gratefully acknowledged for their hard work in the field. H. Hohti and the Finnish Meteorological Institute kindly provided the rainfall radar images. I. Hanski, J.Antonovics, and R. Penczykowski provided valuable comments on the manuscript. This work was supported by funding from the Academy of Finland (grant nos. 250444, 136393, and 133499) and the European Research Council (Independent Starting grant PATHEVOL; 281517) to A.L.L.
The data presented in this paper are deposited in Dryad (10.5061/dryad.vf210).

SUPPLEMENTARY MATERIALS

www.sciencemag.org/content/344/6189/1289/suppl/DC1
Materials and Methods
Supplementary Text
Figs. S1 to S5
Tables S1 to S4
References (*32*–*47*)

19 March 2014; accepted 6 May 2014
10.1126/science.1253621

COMPARATIVE BEHAVIOR

Anxiety-like behavior in crayfish is controlled by serotonin

Pascal Fossat,[1,2] Julien Bacqué-Cazenave,[1,2] Philippe De Deurwaerdère,[1,3] Jean-Paul Delbecque,[1,2]* Daniel Cattaert[1,2]*†

Anxiety, a behavioral consequence of stress, has been characterized in humans and some vertebrates, but not invertebrates. Here, we demonstrate that after exposure to stress, crayfish sustainably avoided the aversive illuminated arms of an aquatic plus-maze. This behavior was correlated with an increase in brain serotonin and was abolished by the injection of the benzodiazepine anxiolytic chlordiazepoxide. Serotonin injection into unstressed crayfish induced avoidance; again, this effect was reversed by injection with chlordiazepoxide. Our results demonstrate that crayfish exhibit a form of anxiety similar to that described in vertebrates, suggesting the conservation of several underlying mechanisms during evolution. Analyses of this ancestral behavior in a simple model reveal a new route to understanding anxiety and may alter our conceptions of the emotional status of invertebrates.

Sources of stress or danger (called stressors) provoke fear, a basic emotion, and generate immediate responses, such as escape, freezing, or aggression. Stress can also lead to anxiety, a more complex state that is considered a secondary emotion because it occurs when the stressor is absent or not clearly identified (*1*–*3*). In humans and rodents, anxiety is experienced as an anticipatory fear that facilitates coping with unexpected situations and

Ecological and evolutionary effects of fragmentation on infectious disease dynamics

Jussi Jousimo *et al.*

Science **344**, 1289 (2014);
DOI: 10.1126/science.1253621